# CHAPTER 34

# Numerical Validation of Directional Wavemaker Theory with Sidewall Reflections

**E.P.D. Mansard,* M.D. Miles* and R.A. Dalrymple†**

## ABSTRACT

A directional wavemaker theory has been developed by Dalrymple to produce a desired oblique planar wave train at any cross-section in the basin. This theory, which uses the reflections from the sidewalls of the basin, can also account for slowly varying depths. This paper describes a numerical validation of this theory, for the constant depth situation, by a wave diffraction model that was recently verified through an extensive series of experimental investigations.

## 1.0 INTRODUCTION

To generate a specified multidirectional wave field in a laboratory basin, the board motions of a segmented wave generator are generally computed on the basis of the snake principle. Although this technique is being used extensively, it has some limitations. For instance, it cannot account for the effects of reflection from sidewalls and the diffraction due to a segmented wave generator of finite length. Also, the size of the optimal testing area inside the model basin that results from this technique can be quite small, particularly if the maximum angle of directional spread is large. In order to overcome some of these limitations, research has been under way in leading hydraulics laboratories around the world into improved techniques for the simulation of multidirectional waves.

Funke & Miles (1987) developed an extension of the snake principle which can be used to obtain a larger useful working area in a multidirectional wave basin. This technique, known as the corner reflection method, makes use of intentional reflections from partial sidewalls about 5m long on both sides of the basin, extending from each end of the wave generator. Like the snake principle itself, however, waves generated by this method are still subject to wave diffraction errors.

*Senior Research Officer, National Research Council of Canada
†Director, Center for Applied Coastal Research, University of Delaware, U.S.A.

Recently, Dalrymple (1989) developed a technique by which an oblique planar wave train of any desired angle of incidence can be generated at any pre-selected cross-section in the basin. This technique was based on a splitting procedure used on the mild slope equation to develop a propagation equation for the wave potential within a wave basin with reflecting sidewalls and a bottom which may have a slope in the direction perpendicular to the wave generator. The resulting equation was solved analytically to determine the wave fields as a function of distance from the generator segments, given their motions.

The major advantage of the Dalrymple theory is that diffraction, refraction and shoaling processes are all properly accounted for, within the realm of linear wave theory. It is also possible to use this technique to calculate the segmented wave generator paddle motions required to produce a pure full-width oblique plane wave train at a specified distance, $D$, from the wavemaker. Multidirectional wave fields are typically generated by the linear superposition of many oblique plane wave components. If the Dalrymple theory is used to generate each component, instead of the snake principle, then the area of the basin where the desired multidirectional wave field can be accurately reproduced will be much larger.

The analytic solution used in the Dalrymple method is only applicable to the case of a wave basin with full-length reflecting sidewalls. The desired oblique plane waves are obtained only at the specified distance $D$ from the wavemaker. As the waves propagate further down the basin, they gradually become contaminated by diffraction and reflection from the sidewalls. The undesired reflection effects can be avoided by using side absorbers at distances greater than $D$, although diffraction effects will still occur. In many model testing applications, the use of partial-length sidewalls is also necessary to reduce errors which would otherwise be caused by sidewall reflection of the diffracted wave field produced by the structure being tested.

It was therefore decided to carry out a numerical study to investigate the performance of the Dalrymple method in a typical multidirectional wave basin with partial-length sidewalls. Wave paddle motions were calculated by the Dalrymple method and the resulting wave field in the basin was then computed by using the linear diffraction model developed by Isaacson (1989). This model can calculate the wave field at any position in the basin, whereas the Dalrymple theory can only be used in the region between the reflecting sidewalls. Another reason for choosing the Isaacson model was that it has recently been verified by extensive experiments in a directional wave basin by Hiraishi et al. (1991). The present numerical study was restricted to the case of a constant depth basin because the Isaacson model cannot be used for a basin with a sloping bottom. In addition to investigating partial-length sidewall effects, the Isaacson model also provided an independent verification of the paddle motions predicted by the Dalrymple method.

## 2.0 THEORETICAL BACKGROUND OF DALRYMPLE'S THEORY

A brief description of Dalrymple's theory is outlined here. Dalrymple (1989) contains a more detailed presentation.

The wave basin is rectangular with width $2b$. The co-ordinate axes are located at the centre of the wave generator with the $y$ axis directed along the generator and the $x$ axis directed prependicularly into the basin. The sidewalls of the basin at $y = \pm b$ are impermeable.

The mathematical theory used in this model follows the treatment of Dalrymple and Kirby (1988) for the combined diffraction and refraction of waves on sloping beaches. The assumed linear water wave motion is described by a velocity potential satisfying the mild slope equation. This mild slope equation, which governs the progressive wave mode and neglects the evanescent wave mode, can be written as:

$$\Phi(x, y, z, t) = \phi(x, y) \frac{\cosh k(h + z)}{\cosh kh} \cdot e^{-i\omega t} \tag{1}$$

$$\frac{\partial}{\partial x}\left(CC_g \frac{\partial \phi}{\partial x}\right) + CC_g \frac{\partial^2 \phi}{\partial y^2} + k^2 CC_g \phi = 0 \tag{2}$$

where $CC_g$ is the product of the wave phase velocity and group velocity. The wave number, $k$, is related to the water depth, $h(x)$, and the angular wave frequency, $\omega$, by the linear dispersion relationship.

The above equations are consistent with small amplitude assumptions and the imposition of a mild bottom slope. At the sidewalls of the basin ($y = \pm b$), there is no flow normal to the walls. Therefore,

$$\frac{\partial \phi}{\partial y} = 0 \quad \text{on} \quad y = \pm b \quad . \tag{3}$$

To satisfy these two lateral boundary conditions,

$$\phi(x, y) = \hat{\phi}(x) \sum_{n=0}^{\infty} (a_n \cos \lambda_n y + b_n \sin \gamma_n y) \tag{4}$$

where $\lambda_n = (n\pi/b)$ and $\gamma_n = (n + \frac{1}{2})\pi/b$ for $n = 0, 1, 2, \ldots, \infty$ .

The reduced mild slope equation becomes two equations:

$$\frac{\partial}{\partial x}\left(CC_g \frac{\partial \hat{\phi}}{\partial x}\right) + CC_g (k^2 - \alpha^2)\, \hat{\phi} = 0 \tag{5}$$

where $\alpha = \lambda_n$ or $\gamma_n$ depending on which of the forms of the solution in Equation (4) is used.

The reduced wave potential, $\hat{\phi}$, can consist of waves propagating in the positive and negative $x$ directions, i.e. $\phi^+$ and $\phi^-$. Adopting the splitting procedure, assuming the reflected waves to be small and, therefore, neglecting the negative potential $\phi^-$, the total forward propagating velocity potential can be written as:

$$\Phi(x,y,z,t) = (\phi_e^+ + \phi_o^+)\frac{\cosh k(h+z)}{\cosh kh} e^{-i\omega t} \tag{6}$$

where

$$\phi_e^+ = \sum_{n=0}^{\infty} A_{n0}\, K_{sr}(x,\lambda_n)\, e^{i\int_0^x \sqrt{k^2-\lambda_n^2}\,dx} \cos \lambda_n y \tag{7}$$

$$\phi_o^+ = \sum_{n=0}^{\infty} B_{n0}\, K_{sr}(x,\gamma_n)\, e^{i\int_0^x \sqrt{k^2-\gamma_n^2}\,dx} \sin \gamma_n y \tag{8}$$

and $K_{sr}$ is the product of the shoaling and refraction coefficients. The subscripts $e$ and $o$ refer to even and odd solutions about the $y = 0$ axis. Some of the "progressive" waves are evanescent, those for which $\lambda_n$ or $\gamma_n > k(x)$. In most cases, when only the far wave field is required, the largest value of $n$ to be retained in the summation is only on the order of 10–20. Although the solution for the velocity potential, $\phi$, is analytic, the phase integrals are determined numerically by the Euler integration method.

In the parabolic forms of the equation, the condition at the wave paddles ($x = 0$) is an initial condition that forces the wave-induced water motions (defined by $\partial\phi/\partial x$) to match the motion of each wave paddle.

The wave paddle motion is assumed to have a linear phase shift along the $y$ axis, leading to the generation of a plane wave train with an angle of incidence, $\theta$, with respect to the $x$ axis. Thus, the paddle motion will be described by the real part of

$$X = S_0\, g(z)\, e^{i(\lambda_0 y - \omega t)} \tag{9}$$

where $g(z)$ is the vertical dependence of the paddle motion over the water depth, $\lambda_0 = k \sin\theta$ is the $y$-component of the wave number of the desired wave and $S_0$ is the maximum amplitude of the paddle stroke at the mean free surface.

The linearized initial condition for this wave generator, in terms of the horizontal velocity in the $x$ direction, is specified by even and odd contributions about the $y$-axis. Now matching the even and odd solutions to the horizontal velocity determined from the velocity potential at $x = 0$, and exploiting various orthogonal properties of the functions that occur in this problem, the expressions for the coefficients $A_{n0}$ and $B_{n0}$ simplify to:

$$A_{n0} = -\frac{2(-1)^n\, S_0\, \omega\, G\, \lambda_0\, \sin(\lambda_0 b)}{(\lambda_0^2 - \lambda_n^2)\sqrt{k^2-\lambda_n^2}\; b} \tag{10}$$

and

$$B_{n0} = -\frac{2i(-1)^n\, S_0\, \omega\, G\, \lambda_0\, \cos(\lambda_0 b)}{(\lambda_0^2 - \gamma_n^2)\sqrt{k^2-\gamma_n^2}\; b} \tag{11}$$

for the case of a wave generator spanning the full width of the basin.

The wave field generated in the basin, for a given set of paddle motions, can be computed with these expressions. Alternatively, if it is required to produce a desired oblique plane wave train extending across the full width of the basin at a given $x$ location, this can easily be done by determining the initial coefficients $A_{n0}$ and $B_{n0}$, not at $x = 0$ as before, but at the desired location $x = x_D$. This yields new values of the coefficients

$$A'_{n0} = \frac{A_{n0}\, e^{i \int_0^{x_D} \sqrt{k^2-\lambda_0^2}\, dx}}{K_{sr}(x_D, \lambda_n)\, e^{i \int_0^{x_D} \sqrt{k^2-\lambda_n^2}\, dx}} \tag{12}$$

and

$$B'_{n0} = \frac{B_{n0}\, e^{i \int_0^{x_D} \sqrt{k^2-\lambda_0^2}\, dx}}{K_{sr}(x_D, \gamma_n)\, e^{i \int_0^{x_D} \sqrt{k^2-\gamma_n^2}\, dx}} \tag{13}$$

where $\lambda_0$ is evaluated at $x_D$. The wave paddle motion is now obtained from Equations 7 and 8 evaluated at $x = 0$, resulting in the summation of various sinusoidal motions.

Although Dalrymple (1989) provides some preliminary validation of this technique using the same theory, a more detailed validation has been carried out in this study using the Isaacson (1989) diffraction model, which has recently been verified by an extensive set of physical experiments. A brief description of the Isaacson model and its experimental verification is given below.

## 3.0 THEORETICAL BACKGROUND OF THE ISAACSON MODEL

This model was developed by Isaacson (1989) to predict the wave field in a multidirectional wave basin. It is based on linear wave diffraction theory and uses a boundary element representation of the segmented wave generator and the reflecting walls of the basin.

Isaacson defines a velocity potential satisfying the Helmholtz equation within the fluid region and the boundary conditions along the generator faces and any specified reflecting walls. A suitable radiation condition is also applied so that the remaining parts of the wave basin boundary are treated as perfect wave absorbers.

The potential $\phi$ may be expressed as the potential due to a distribution of point wave sources along the generator faces and any reflecting boundaries. Thus,

$$\phi(\mathrm{x}) = \frac{1}{4\pi} \int_S f(\xi)\, G(\mathrm{x};\xi)\, dS \tag{14}$$

where $S$ denotes the horizontal contour along the generator faces and fixed walls and $f(\xi)$ represents the source strength distribution function. $G(\mathrm{x};\xi)$ is a Green's function for the potential at an arbitrary point $\mathrm{x}$ due to a point wave source located at the point $\xi$ on $S$, and $dS$ denotes a differential length along $S$.

The boundary condition along $S$ equates the flow velocity component normal to $S$ to the wave paddle velocity along a generator face and to zero along a reflecting wall. This gives an integral equation for $f(\xi)$ which is then solved by using a discrete representation of the horizontal contour, $S$, with a finite number of short straight elements and assuming the source strength to be constant over each element. Using this approximation, the integral equation is satisfied at the centre of each boundary element and is thus reduced to a set of linear equations for the source strengths. The velocity potential, $\phi$, is obtained from the solution of these equations and a discrete version of Equation 14. Once the potential is known, the height and the phase angle of the waves at any point in the basin can be calculated easily.

The most important parameter in this numerical model is the total number of discrete boundary elements that are required to predict the wave field in the basin. Reducing the boundary element length increases the accuracy of the predicted wave field but eventually leads to excessive computational effort. Hiraishi et al. (1991) undertook a numerical investigation to determine the optimum ratio of boundary element length to wave length required to obtain reliable results. These predictions were subsequently validated by an extensive experimental program.

## 4.0 EXPERIMENTAL VALIDATION OF THE ISAACSON MODEL

The amplitudes and phases of wave trains predicted by this diffraction model for different combinations of wave periods and angles of incidence, were compared to measurements made at more than 200 locations in a test basin. A brief description of this experimental investigation is given below.

The experiments were carried out in the multidirectional wave basin of the NRC Hydraulics Laboratory, which has a length of nearly 20m and a width of 30m. A segmented wave generator consisting of 60 segments, each with a width of 0.5m is located along one 30m side of the basin.

Perforated sheet metal wave absorbers, developed by the NRC Hydraulics Laboratory to yield less than 5% reflection, were installed along the other three sides of the basin. Removable sidewalls could be used to cover the side absorbers, either totally or partially.

In order to scan the sea states prevailing at different locations in the basin, a steel frame was designed to accommodate nineteen wave gauges. This steel frame, shown in Figure 1, was suspended at a single point from a hoist which was in turn attached to a trolley. This trolley ran, through remote-control, on a track under the ceiling over the centre of the basin aligned in a direction normal to the face of the wave generator. The frame could also be rotated about its suspension point to make simultaneous measurements of wave profiles along a line parallel to the crest of an oblique wave.

Validation of the Isaacson diffraction model was carried out using both long-

Figure 1: Photograph of Steel Frame with Wave Gauges

crested normal and oblique regular waves. Waves with periods ranging from 1.5s to 2.25s were produced by the snake principle and also by the NRC corner reflection method, using short reflecting sidewalls of approximately 5m length.

Since the Isaacson model is based on linear theory, wave heights were kept under 20cm. For each sea state, wave measurements at different cross-sections in the basin were carried out by relocating the 19-probe frame at different target positions. At each position, wave generation and data sampling were exercised for 180s. In order to correlate measurements made at the various cross-sections in the basin, the data acquisition was synchronized with the activation of the wave generator. A large number of tests was carried out to ensure repeatability of the sea states. Sufficient time was allowed for the oscillations in the basin to settle down between successive tests. While a detailed presentation of these investigations can be found in Hiraishi et al. (1991), one example of the comparison between numerical and physical model results is presented here.

The points in Figure 2a show the wave height distribution realized at three different measurement lines, as well as the corresponding numerical predictions, for 2s waves propagating in a line parallel to the wave generator. The distances of these lines, measured from the wave paddles and expressed as $X_c$, are indicated in the figure.

Figure 2b illustrates results of oblique waves with $\theta = 30°$, measured in a line parallel to the wave generator (i.e. $\alpha = 0°$) and parallel to the crest line ($\alpha = 30°$). For the sake of easier comparison, the measured wave heights, $H$, are normalized

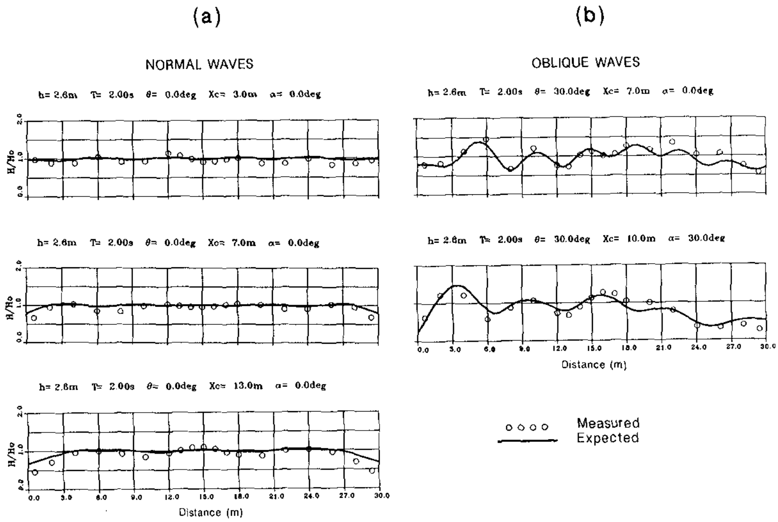


Figure 2: Comparison of Measured and Predicted Waves for Isaacson Model

with respect to the target heights, $H_0$. It can be seen from this figure that the measured wave heights agree reasonably well with the predicted ones. Similar cases of good agreement were found for all periods except one that stimulated cross-mode waves in the experimental basin. Interested readers should refer to Hiraishi et al. (1991) for a complete presentation of the results.

Based on these experimental investigations, it was concluded that the Isaacson numerical model can predict the generated wave field quite well for a specified basin layout and a specified set of segmented wave generator paddle motions.

## 5.0 VALIDATION OF DALRYMPLE'S THEORY

### 5.1 Validation Procedure

Since the Isaacson diffraction model has been extensively validated by the experiments described above, it was decided to use it to assess the effectiveness of the Dalrymple method. Although Dalrymple's theory itself can be used to predict the water surface elevation, this can only be done in the region between the reflecting sidewalls. Since the wave field at the wavemaker is rather complex for the Dalrymple method, the accuracy of the oblique plane wave produced may also be limited by the finite width of the wavemaker segments. The Isaacson model allows the wave field to be calculated at all points in a basin of constant depth, and also can model the effects of finite segment width.

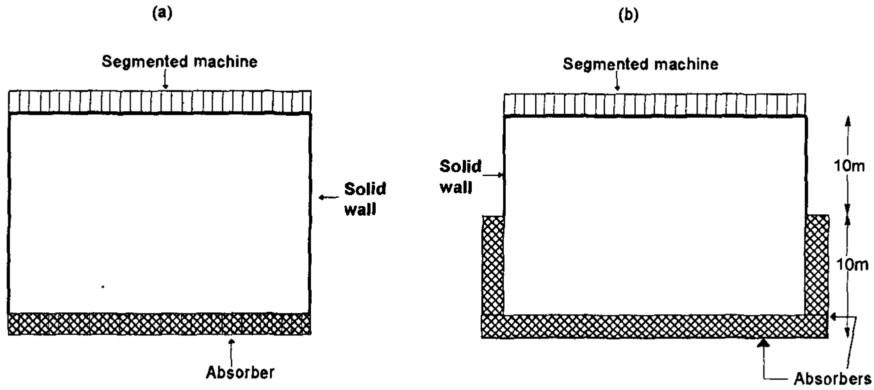


Figure 3: Layout of Basins for Verification of Dalrymple's Theory

In view of these considerations, the following procedure was used to investigate the performance of the Dalrymple method in a typical wave basin:

- Use Dalrymple's theory to estimate the required paddle motions of the segmented wave generator for the reproduction of a given sea state at the desired location.
- Use the computed motions as inputs to the Isaacson diffraction model to predict the wave field inside the test basin and determine how accurately the desired sea state can be realized at various locations.

The layouts of the basin used in this numerical procedure are shown in Figure 3. These layouts correspond to the NRC Hydraulics Laboratory basin described above. Two different cases of sidewall lengths were chosen for this study. Figure 3a represents the situation where the two sides are covered fully with reflecting walls, while Figure 3b corresponds to sidewalls extending only 10m from the paddles; the remaining 10 metres on each side consist of absorbers. In both cases, the wavemaker was assumed to have a segment width of 0.5m.

According to Dalrymple's theory, it is possible to reproduce a desired oblique wave train at any cross-section in the basin up to the limit of the reflecting sidewalls. Consequently, the desired wave train can be produced at any distance from 0 to 20m from the wavemaker in the layout of Figure 3a but only at distances between 0 and 10m for the case of Figure 3b.

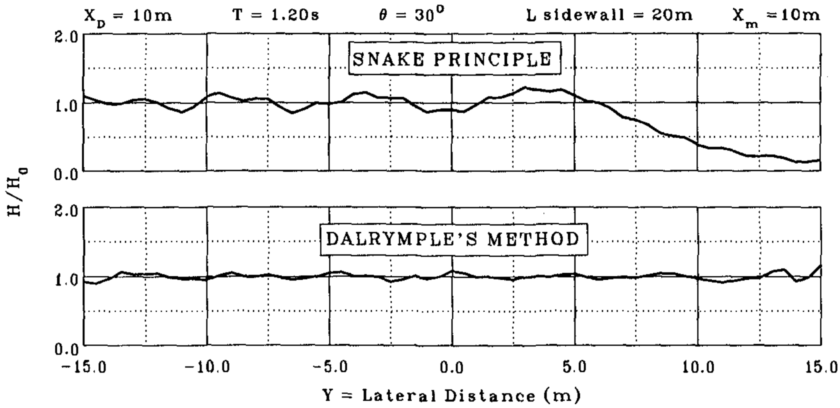


Figure 4: Wave Height Distributions at $x_D = 10$m for Snake Principle and Dalrymple Method

## 5.2 Results of the Validation Procedure

### 5.2.1 Full-length sidewalls

A comparison of the snake principle with no sidewalls and the Dalrymple method with full-length sidewalls is shown in Figure 4 for a wave train with a period of $T = 1.2$s and a propagation angle of $\theta = 30°$. The wave height distributions for both methods were calculated by the Isaacson model. It can be seen that wave height uniformity is greatly improved with the Dalrymple method, not only in the main diffraction zone at the right, but in the centre of the basin as well.

Wave height distributions, at various distances from the wavemaker, are shown in Figure 5 for the basin layout shown in Figure 3a. These were predicted by the Isaacson model using the paddle motions computed by Dalrymple's theory. In Figure 5a, the target sea state is a wave train with a period of $T = 0.75$s and a propagation angle of $\theta = 15°$. In Figure 5b, the target wave train has a period of $T = 1.20$s and a propagation angle of $\theta = 30°$. In both cases, the reproduction distance, $x_D$, is 10m.

These figures demonstrate the capability of Dalrymple's method. It is interesting to note the complexity of the wave field that is required to be produced near the paddles to simulate the desired water surface elevation at the specified locations. Similarly, the influence on the wave field of the reflection from the solid walls extending beyond 10m can also be appreciated.

### 5.2.2 Partial-length sidewalls

Figure 6 illustrates results similar to those in Figure 5 but for the basin layout depicted in Figure 3b. A target wave train with $T = 0.75$s and $\theta = 15°$ was used and wave fields were calculated for two different reproduction distances, $x_D$. The results for $x_D = 5$m and $x_D = 10$m are shown in Figures 6a and 6b, respectively. Figure 6b is particularly interesting since it shows the ability to reproduce the desired sea state at the end of the sidewalls. As expected, the absorbers located beyond the 10m limit of the sidewalls help eliminate the reflections, thus ensuring a reasonably good wave field, even beyond the 10m distance.

Once again, these figures illustrate the validity of Dalrymple's theory. It should be noted that, although the water surface elevation realized at the desired locations is very good, a small variability (less than 5%) seems to exist and tends to increase with wave period. Research is continuing to investigate the reasons for this variability. Possible causes include finite segment width effects and the truncation point used for the summations in the Dalrymple theory (e.g. Equations 7 and 8).

## 6.0 SIZE OF AREA WITH HOMOGENEOUS SEA STATES

For model studies of offshore or coastal structures, it is important to ensure that a large area with a homogeneous sea state is available for testing purposes. For this reason, it is of interest to estimate the size of homogeneous area that can be obtained using Dalrymple's theory.

An example of this is shown in Figure 7 which illustrates the boundary inside the wave basin where the wave heights can be expected to be within $\pm 10\%$ of the target wave height, $H_0$. The two basin layouts shown in Figure 3 have been used. The thick line shows the result for full-length reflecting sidewalls, while the dashed line shows the case of partial-length sidewalls. The sea states illustrated in Figure 5b were used in these calculations for the full-length sidewall case.

It can be seen that the homogeneous area extends over the full width of the basin at the reference distance of $x_D = 10$m, where the target wave train was to be reproduced. At larger $x$ distances, the width of the homogeneous zone gradually decreases. In this case, it is better to use a 10m sidewall on one side to prevent reflection when $x > x_D$ and a 20m sidewall on the opposite side to reduce diffraction effects. However, in the general multidirectional case, with waves propagating in both positive and negative directions, it would be best to use partial-length sidewalls on both sides. More calculations of this kind are under way in order to determine the optimum sidewall length for various multidirectional wave situations.

## 7.0 CONCLUSIONS

Dalrymple has proposed a theoretical model to reproduce a planar, oblique wave train at any predetermined cross-section in a multidirectional basin. This theory, which uses reflections from sidewalls and the mild slope equation for varying water depth, was validated numerically for a constant depth situation using the Isaacson diffraction model. The results indicate that Dalrymple's method is indeed a

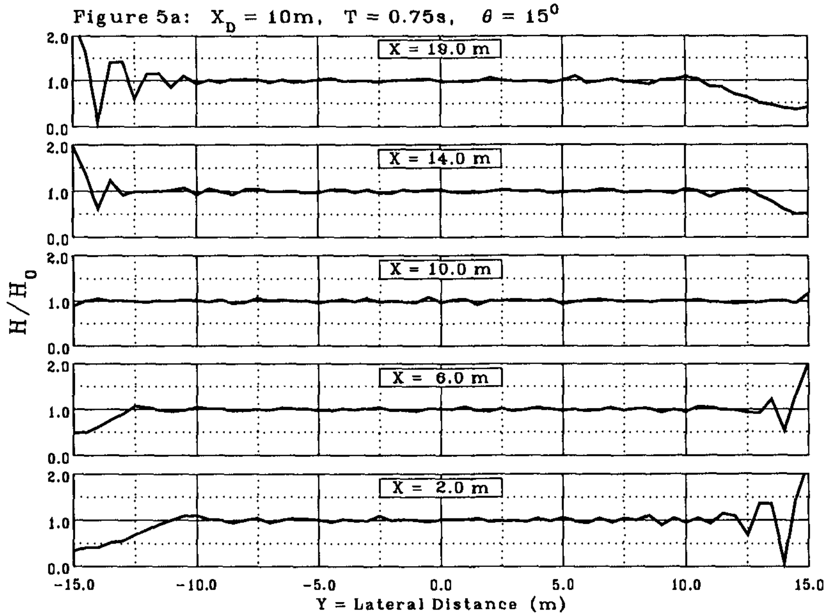


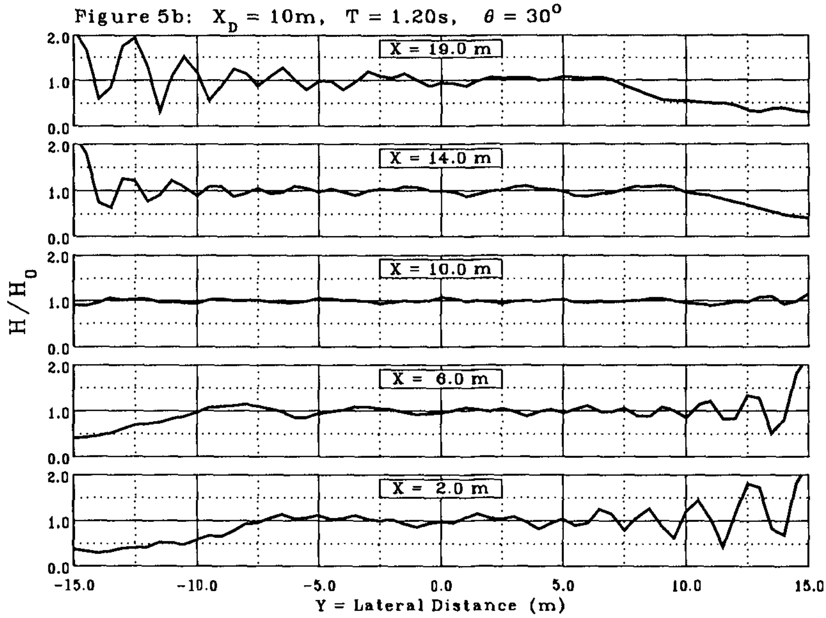


Figure 5: Dalrymple Method Wave Height Distributions for 20m Sidewalls at Various $X$ Distances from the Wavemaker.

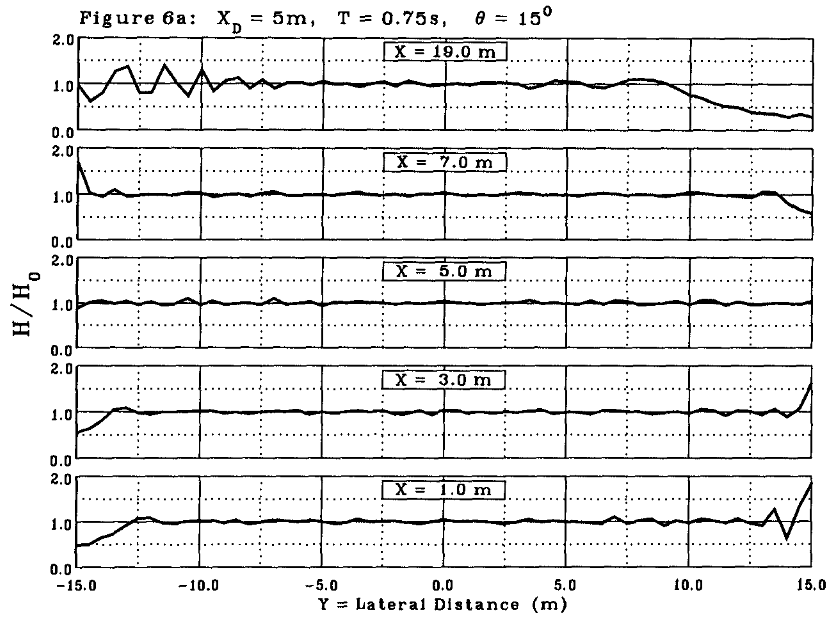


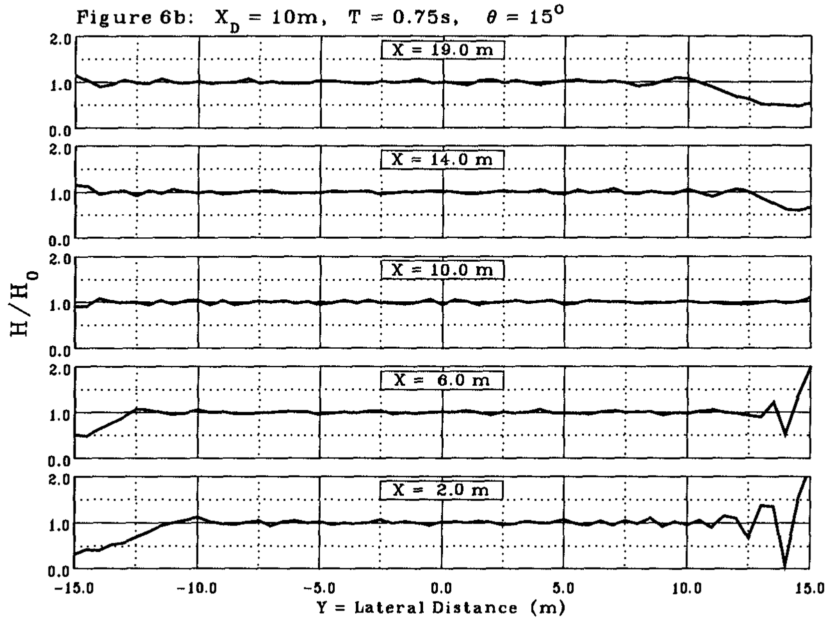


Figure 6: Dalrymple Method Wave Height Distributions for 10m Sidewalls at Various $X$ Distances from the Wavemaker.

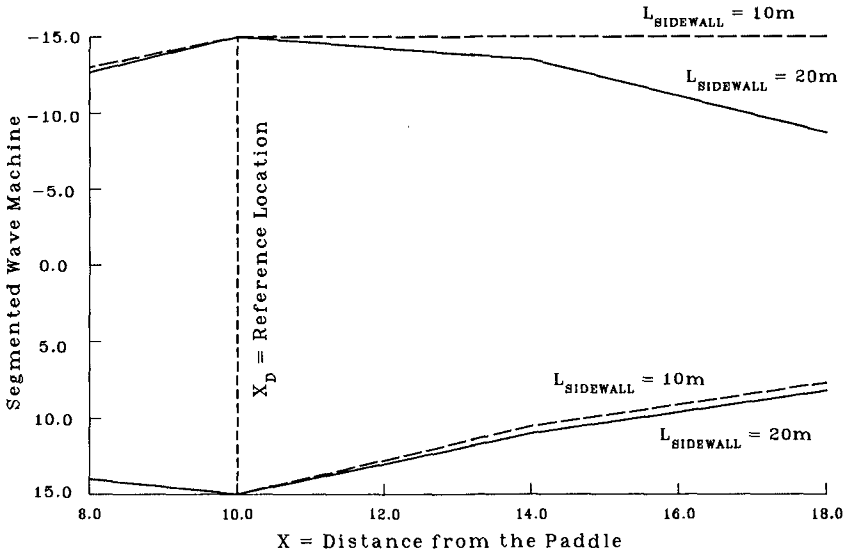


Figure 7: Size of Area with ±10% Uniformity for $T$ = 1.20s and $\theta = 30°$

powerful tool that can enhance the model testing capability of a multidirectional wave basin. Further work is planned at NRC to evaluate the Dalrymple method experimentally in a basin with a sloping bottom.

## 8.0 REFERENCES


Dalrymple, R.A. and Kirby, J.T. (1988). *Very Wide Angle Water Wave Models and Wave Diffraction*, Journal of Fluid Mechanics, 192, pp. 33–50.

Funke. E.R. and Miles. M.D. (1987). *Multidirectional Wave Generation with Corner Reflectors*, Technical Report TR-HY-021, Division of Mechanical Engineering, National Research Council of Canada.

Isaacson, M. (1989). *Prediction of Directional Waves Due to a Segmented Wave Generator*, Proc. 23rd IAHR Congress, Ottawa, Canada. August 21–25, Vol. C. pp. 435–442.

Dalrymple, R.A. (1989). *Directional Wavemaker Theory With Sidewall Reflection*, Journal of Hydraulic Research, Vol. 27, No. 1, pp. 23–34.

Hiraishi, T., Mansard, E.P.D., Miles, M.D., Funke, E.R. and Isaacson, M., (1991). *Validation of a Numerical Diffraction Model for Multidirectional Wave Generation*, Hydraulics Laboratory Technical Report TR-HY-037, National Research Council of Canada.